の分化増殖・生存を制御している。CSF 14-3-3 はプリオン病診断特異的マーカーとして有用であるが、MS においても 14-3-3, tau, neurofilament proteins は、急速な脳組織の破壊の際に CSF 中に遊出し、axonal injury のマーカーとなる可能性がある(*Satoh et al. J Neurol Sci* 2003; **212**: 11-20)。

4. DNA マイクロアレイによる MS の診断

DNA マイクロアレイは、スライドグラス基盤上に数万遺伝子のオリゴヌクレオチドを高密度に固定したチップで、個々の細胞における全遺伝子発現情報(transcriptome)や遺伝子多型(single nucleotide polymorphism; SNP)を包括的に解析出来るツールである。近年マイクロアレイによる網羅的解析が、MS の発症リスク評価、鑑別診断、再発予測、IFNB 治療反応性予測のために応用されている。例えば MS 931 家系(family trios)がジェノタイピングアレイを用いて解析され、発症リスク関連遺伝子として ILR2A, ILR7A の SNP が同定された(The International Multiple Sclerosis Genetics Consortium. *N Engl J Med* 2007; **357**: 851-862)。マイクロアレイ解析の原理とわれわれ研究成果[10]に関しては、「Mini Lecture DNA マイクロアレイ」の項を参照されたい。以下国外における MS リンパ球の遺伝子発現解析研究の現況を概説する。

Bomprezzi らは、RRMS 患者(n = 27)と健常者(n = 19)の peripheral blood mononuclear cells(PBMC)で発現差異を示す 53 遺伝子を同定し、MS における T 細胞活性化関連遺伝子 IL-7R, ZAP70, TNFRSF7 の発現上昇を報告した(*Hum Mol Genet* 2003; **12**: 2191-2199)。Achiron らは、RRMS 患者(n = 26)と健常者(n = 18)の PBMC の遺伝子発現プロフィールを比較し、両群間で 1,109 遺伝子の発現差異を認め、MS における T 細胞活性化関連遺伝子 LEF1, TCF3, SLAM, ITGB2, CTSB の上昇を報告した(*Ann Neurol* 2004; **55**: 410-417)。しかし MS 14 例では採血時に IFNB, glatiramer acetate, intravenous immunoglobulins を投与中であり、治療薬が遺伝子発現に直接影響している可能性がある。Corvol らは、CIS 患者(n = 37)の $CD4^+$ T 細胞で、患者群を 4 群に分類する 975 遺伝子を同定し、T 細胞増殖抑制因子 TOB1 の発現低下が CDMS への移行のマーカーとなることを報告した(*Proc Natl Acad Sci USA* 2008; **105**: 11839-11844)。Gurevich らは、未治療 RRMS 患者(n = 62)と CIS 患者(n = 32)の PBMC の遺伝子発現プロフィールを比較し、500 日以内または 50 日以内の再発を予測する遺伝子セット first level predictors (FTP), fine tuning predictors (FTP)を同定した(*BMC Med Genet* 2009; **2**: 46)。再発予測遺伝子には、TGFB2 シグナル伝達系遺伝子が多く含まれていた。Archiron らは、9 年間の追跡期間中に、MS を発症した群

(MS-to-be; n = 9)とMSを発症しなかった群(MS-free; n=11)のPBMCの遺伝子発現プロフィールを比較し、MS前駆病態(preactive stage of MS)において、T細胞アポトーシス誘導因子NR4A1の発現低下を認めた(*Neurobiol Dis* 2010; **38**: 201-209)。Brynedalらは、RRMS患者(n =26)のCSF細胞とPBMCのペアで遺伝子発現プロフィールを比較し、再発期にPBMCでは266遺伝子が発現変動したが、CSF細胞では顕著な変動が見られなかった(*Neurobiol Dis* 2010; **37**: 613-621)。

PBMCではIFNB治療を開始すると数時間以内に、プロモーターにIFN-stimulated response element(ISRE)を有するIFNB応答遺伝子(IFN-responsive genes; IRG)の発現が上昇する(Weinstock-Guttman *et al. J Immunol* 2003; **171**: 2694-2702)。Stürzebecherらは、RRMS患者(n = 10)で、IFNB治療前後にPBMCの遺伝子発現プロフィールを解析し、IFNBレスポンダーで25遺伝子の変動(IFI17, OAS, STAT1などの上昇)を認めた(*Brain* 2003; **126**: 1419-1429)。しかし、彼らは一度凍結保存したリンパ球を解凍してから解析しており、実験操作が遺伝子発現に影響した可能性を否定出来ない。Byunらは、ジェノタイピングアレイを用いて、RRMS患者(n = 206)のIFNBレスポンダーとノンレスポンダーを識別するHAPLN1, GPC5, COL25A1, CAST, NPAS3のSNPを同定した(*Arch Neurol* 2008; **65**: 337-344)。Comabellaらは、RRMS患者(n = 47)のうちIFNBノンレスポンダーのPBMCでは、治療前からIRGの発現亢進を認めた(*Brain* 2009; **132**: 3353-3365)。Sellebjergらは、IFNB中和抗体陽性者のPBMCで、IRG発現誘導の低下を認めた (*Eur J Neurol* 2009; **16**: 1291-1298)。Gertschesらは、RRMS患者(n = 25)のPBMCではIFNB治療により、STAT1を中心とする遺伝子ネットワークの発現上昇とITGA2Bを中心とする遺伝子ネットワークの発現低下を認めることを報告した(*Pharmacogenomics* 2010; **11**: 147-161)。

マイクロRNA(microRNA; miRNA)は、ゲノムにコードされた約22塩基からなるnon-coding RNAであり、標的となる遺伝子mRNAの3'-untranslated regionに存在する配列に、不完全な相補性で結合してタンパク質の翻訳を抑制するか、完全な相補性で結合してmRNAを分解する。現在までに、ヒトでは1000種類以上のmiRNAが同定されている。その多くは進化を通じてよく保存されており、発現は時間的空間的に制御され、発生・癌化・細胞死・免疫制御において、重要な役割を果たしている。未治療MS患者末梢血では、T細胞活性化遺伝子群の発現を抑制するmiR-17とmiR-20aの発現が低下している(Cox *et al. PLoS One* 2010; **5**: e12132)。他にもMS末梢血特異的miRNAとしてmiR-145(Keller *et al. PLoS One* 2009; **4**: e7440), 再発特異的miRNAとしてmiR-18b(Otaegui *et al. PLoS One* 2009; **4**: e6309)などが報告されている。

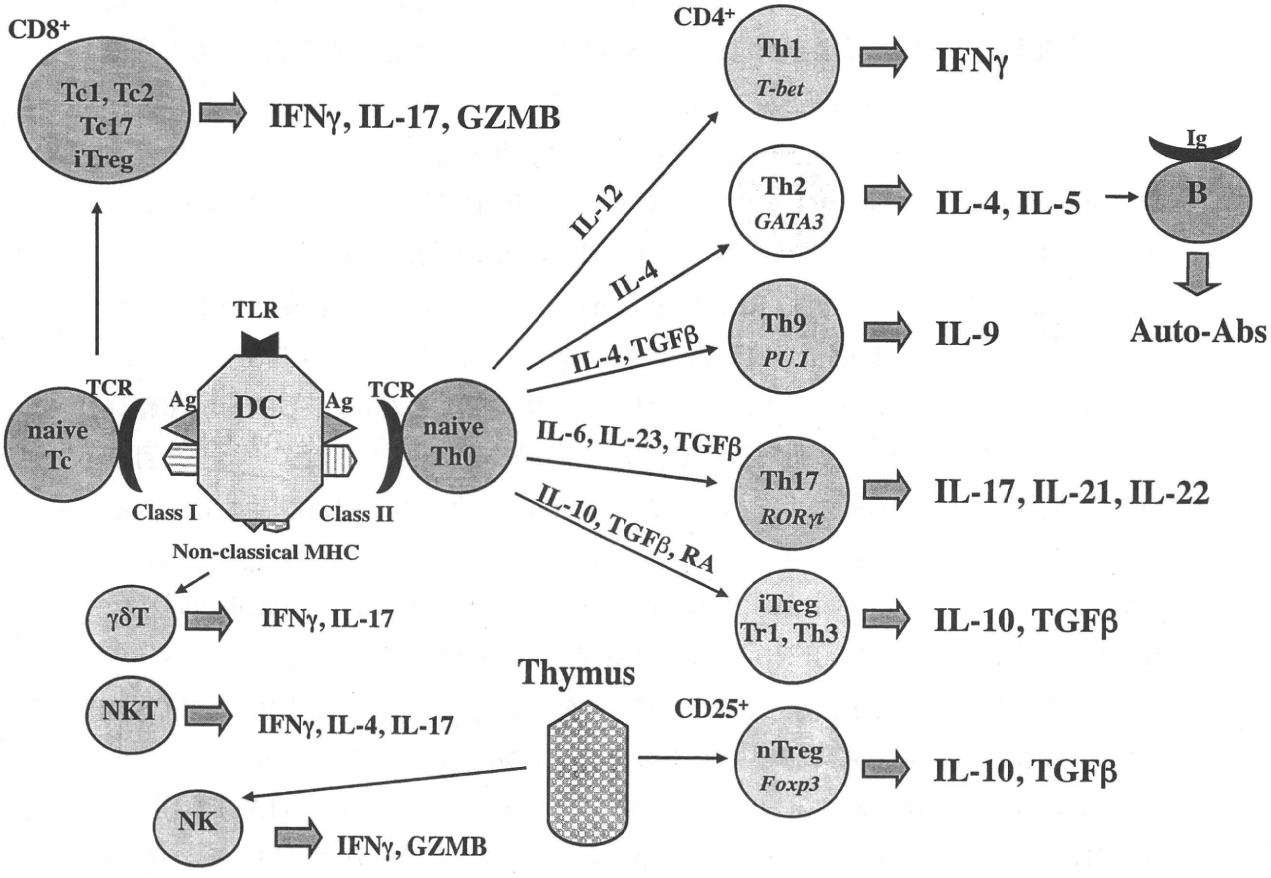
CD8+
Tc1, Tc2
Tc17
iTreg
IFNγ, IL-17, GZMB
TLR
TCR
Ag
DC
Ag
TCR
naive
Tc
naive
Th0
Class I
Class II
Non-classical MHC
γδT
IFNγ, IL-17
NKT
IFNγ, IL-4, IL-17
NK
IFNγ, GZMB
Thymus
CD4+
Th1
T-bet
IFNγ
Th2
GATA3
IL-4, IL-5
Ig
B
Auto-Abs
Th9
PU.1
IL-9
Th17
RORγt
IL-17, IL-21, IL-22
iTreg
Tr1, Th3
IL-10, TGFβ
CD25+
nTreg
Foxp3
IL-10, TGFβ
IL-12
IL-4
IL-4, TGFβ
IL-6, IL-23, TGFβ
IL-10, TGFβ, RA

図1

多発性硬化症(MS)診療のすべて
Mini Lecture

DNA マイクロアレイ

佐藤　準一

明治薬科大学薬学部生命創薬科学科バイオインフォマティクス
〒204-8588 東京都清瀬市野塩 2-522-1
Tel & Fax: 042-495-8678

Jun-ichi Satoh
Department of Bioinformatics, Meiji Pharmaceutical University, 2-522-1 Noshio, Kiyose, Tokyo 204-8588, Japan.
Tel & Fax: 042-495-8678

1. DNA マイクロアレイ解析の意義

2003 年にヒトゲノムプロジェクトが完了し、全ヒト遺伝子約 22,000 の塩基配列が解読された。DNA マイクロアレイは、スライドグラス基盤上に数万遺伝子の cDNA やオリゴヌクレオチドを高密度に固定したチップで、個々の細胞における全遺伝子発現情報(transcriptome)を包括的に解析出来るツールである[1)]。ヒト以外では、既にゲノムプロジェクトが完了している生物種、マウス・ラット・アカゲザル・イヌ・ウシ・イネ・ゼブラフィッシュ・ショウジョウバエ・酵母・線虫・大腸菌でも、マイクロアレイ解析が可能となっている。さらに最近、タンパク質をスライドグラス上に高密度に固定し、タンパク質間相互作用を網羅的に解析可能なプロテインマイクロアレイも登場した[2)]。近年、マイクロアレイを用いた網羅的解析により、癌や神経難病のバイオマーカーや創薬の標的分子が次々明らかにされた。さらに臨床所見や画像のみでは鑑別困難な疾患の補助診断、腫瘍悪性度や予後の予測、薬物応答や副作用の予測、治療効果の判定にも幅広く応用され、テーラメイド医療(personalized medicine)の樹立に必須の研究手法となっている。システム生物学の観点から、ヒトは大規模な分子ネットワークにより精密に構築された複雑系であり、多くの難病がシステム固有のロバストネスの破綻に起因すると考えられている。従って難病の病態解明のためには、ゲノムワイドの分子ネットワーク解析が重要な研究課題となる[3)]。

2. DNA マイクロアレイ解析の原理

DNA マイクロアレイは、cDNA を基盤上にスポッターで固定するスタンフォード方式と、基盤上で直接オリゴヌクレオチドを合成伸長する GeneChip(Affymetrix)に大別される。発現解析アレイ以外には、スプライスバリアントの解析が可能なエクソンアレイ、遺伝子多型や染色体コピー数の解析が可能なジェノタイピングアレイ、chromatin immunoprecipitation(ChIP) on Chip 解析が可能なゲノムタイリングアレイが市販されている。マイクロアレイ解析では、2 種類以上の細胞や組織から mRNA または total RNA を抽出し、T7 RNA 増幅法で増幅する。スタンフォード方式では、比較の対象となる cDNA, cRNA を個別の蛍光色素 Cy3, Cy5 で標識し、同一チップ上で競合的ハイブリダイゼーションを行うため 2 色法と呼ばれる。GeneChip では、cDNA から in vitro transcription 反応によりビオチン標識 cRNA を作成、フラグメントに切断してハイブリダイゼーションを行い、ストレプトアビジン-フィコエリスリンで検出する。1 サンプルに 1 アレイを使用してアレイ間の発現レベルを比較するので 1 色法と呼ばれる。スキャナーで蛍光を検出、シグナル強度を正規化し、サンプル間の遺伝子発現プロフィールを比較

する。グローバルノーマリゼーションは、比較するチップ上の全遺伝子の発現強度の総和が等しいと仮定する正規化法である。DNA マイクロアレイ解析では、一度に多数の遺伝子の発現差異を比較するため、遺伝子毎に t 検定で評価すると、多数の偽陽性遺伝子を拾ってしまう。通常は多重検定を行って Bonferroni 補正を付加するか、偽陽性率(false discovery rate; FDR)を考慮して、統計学的有意差を評価する。

有意な発現変動を示す遺伝子(differentially expressed genes; DEGs)に関しては、発現レベルをリアルタイム RT-PCR で定量的に検証する。さらに Web 上の解析ツール DAVID Bioinformatics Resources 6.7(david.abcc.ncifcrf.gov)や Encyclopedia of Genes and Genomes(KEGG)(www.kegg.jp)を用いて、アノテーションを調べて生物学的な意味付けを行う。KeyMolnet(医薬分子設計研究所)は、専門家が一流のレビューや PubMed から 123,000 種類の生体分子のリレーションに関する情報を収集して構築した knowledgebase であり、アレイデータを入力することにより、最も密接に関連している分子ネットワークを同定することが出来る[4]。

多数のサンプルを比較解析する場合は、データセットの要素特性を分類するために、GeneSpring(Agilent)を用いて階層的クラスター解析を行う。サポートベクターマシン(support vector machine; SVM)は、指標遺伝子(classifier)の抽出に用いたデータを訓練セットとして機械学習することによりパラメータ(Kernel 関数)を選出し、新規のデータセットにおけるクラスターを識別可能な超平面を同定する解析方法である。

3. DNA マイクロアレイによる MS 病型・治療反応性・再発予測マーカーの解析

以下 DNA マイクロアレイによる MS リンパ球の遺伝子発現解析に関するわれわれの研究成果に関して概説する。国外における研究の現況は、「多発性硬化症(MS)の血液診断」の項を参照されたい。

MS は臨床経過から、再発寛解型(relapsing-remitting MS; RRMS), 2 次進行型(secondary progressive MS; SPMS), 1 次進行型(primary progressive MS; PPMS)に分類され、多様な病態を呈する。DNA マイクロアレイは、MS 多様性の分子遺伝学的背景の解析に威力を発揮する。われわれは interferon-beta(IFNB)未治療活動性 MS 患者(n =72; 46 例は初回採血直後から 2 年間 IFNB 治療を開始)と健常者(n = 22)の末梢血 $CD3^+$ T 細胞の遺伝子発現プロフィールを、DNA マイクロアレイ(Hitachi Life Science)で解析した[5,6]。両群間で発現差異を示す上位 30 遺伝子のうち 25 遺伝子が、アポトーシス制御遺伝子に分類され、MS の T 細胞ではアポトーシス促進遺伝子と抑制遺伝子の拮抗的バランスが存在していた[5]。

さらに MS 患者と健常者で有意な発現差異を示す 286 遺伝子を抽出し、KeyMolnet で分子ネットワークを解析し、共通上流として NF-κB を介する遺伝子発現制御系を同定した [7]。NF-κB はサイトカインやケモカインの正の制御転写因子で、炎症の増幅および遷延化に働く。この 286 遺伝子を指標遺伝子として階層的クラスター解析を行い、臨床データとの関連性を評価した(図 1)。286 遺伝子は 5 クラスに分類され、患者群は健常者群から独立したクラスターを形成し、4 サブグループ A, B, C, D に分類された。A 群は軽症例が多く、発現プロフィールが最も健常者に類似し、B 群は臨床的活動性が最も高く、ケモカインが集積しているクラス 5 遺伝子群の発現レベルが最も高く、C 群は大脳限局病変を呈する患者が多く、D 群は Expanded Disability Status Scale(EDSS)スコアが最も高値であった [6]。IFNB 治療を開始した 46 例で、治療前後 2 年間の再発回数・ステロイドパルス日数・入院日数・EDSS・MRI T2 強調画像病巣数・患者の治療満足度をスコア化して、IFNB レスポンダーとノンレスポンダーに分類すると、レスポンダーは A 群と B 群に集積していた [6]。

また peripheral blood mononuclear cells(PBMC)を IFNB で刺激すると、3 時間以内に CXCR3 リガンドケモカイン(CXCL11, CXCL10, CXCL9)と CCR2 リガンドケモカイン(MCP1, MCP2)の発現が、100 倍以上上昇することを見出した [8]。前者は Th1 細胞、後者は単球・マクロファージの遊走を促進し、炎症を増強する。すなわち多数のケモカインが、早期 IFN 応答遺伝子(IFN-responsive genes; IRG)であることがわかった。ケモカインバーストは、IFNB 治療早期副作用である発熱・皮膚潰瘍・肝障害の発現と関連している可能性がある。

さらにハンガリー人一卵性双生児 MS ペア 4 組(MS/MS, MS/MS, MS/MS, MS/健常者)の末梢血 $CD3^+$ T 細胞を DNA マイクロアレイで解析し、MS 特異的 20 遺伝子を同定し、KeyMolnet で分子ネットワークを解析し、共通上流として Ets を介する遺伝子発現制御系を同定した [7]。Ets-1 は Th17 細胞分化の負の制御転写因子である [9]。また RRMS 患者(n = 6)の再発期と寛解期の末梢血 $CD3^+$ T 細胞を DNA マイクロアレイで解析し、再発期特異的 43 遺伝子を同定した [10]。この 43 遺伝子を階層的クラスター解析の指標遺伝子とすると、再発期と寛解期のサンプルを独立したクラスターとして分離出来た。すなわち 43 遺伝子のセットは、MS 再発予測のバイオマーカーとなる可能性がある [10]。

文献

1) 佐藤準一: アレイインフォマティクスの進展. 薬学雑誌 2008; **128**: 1537-1545

2) 佐藤準一: プロトアレイによるタンパク質インターラクトーム解析. 小田吉哉・長野光司(編), 創薬研究のためのタンパク質・プロテオミクス解析技術. 羊土社, 2010; 75-80

3) Satoh J: Bioinformatics approach to identifying molecular biomarkers and networks in multiple sclerosis. *Clin Exp Neuroimmunol* 2010; **1**: 127-140

4) Satoh J, Tabunoki H, Yamamura T: Molecular network of the comprehensive multiple sclerosis brain lesion proteome. *Mult Scler* 2009; **15**: 531-541

5) Satoh J, Nakanishi M, Koike F, *et al.*: Microarray analysis identifies an aberrant expression of apoptosis and DNA damage-regulatory genes in multiple sclerosis. *Neurobiol Dis* 2005; **18**: 537-550

6) Satoh J, Nakanishi M, Koike F, *et al.*: T cell gene expression profiling identifies distinct subgroups of Japanese multiple sclerosis patients. *J Neuroimmunol* 2006; **174**: 108-118

7) Satoh J, Illes Z, Peterfalvi A, *et al.*: Aberrant transcriptional regulatory network in T cells of multiple sclerosis. *Neurosci Lett* 2007; **422**: 30-33

8) Satoh J, Nanri Y, Tabunoki H, *et al.*: Microarray analysis identifies a set of CXCR3 and CCR2 ligand chemokines as early IFNβ-responsive genes in peripheral blood lymphocytes: an implication for IFNβ-related adverse effects in multiple sclerosis. *BMC Neurology* 2006; **6**: 18-34

9) Du C, Liu C, Kang J, *et al.*: MicroRNA miR-326 regulates T_H-17 differentiation and is associated with the pathogenesis of multiple sclerosis. *Nat Immunol* 2009; **10**: 1252-1259

10) Satoh J, Misawa T, Tabunoki H, *et al.*: Molecular network analysis of T-cell transcriptome suggests aberrant regulation of gene expression by NF-κB as a biomarker for relapse of multiple sclerosis. *Dis Markers* 2008; **25**: 27-35

図の説明

図 1. 階層クラスター解析. MS 患者(n =72)と健常者(n = 22)の末梢血 $CD3^+$ T 細胞で有意な発現差異を示す 286 遺伝子を抽出し、指標遺伝子として階層的クラスター解析を行った。286 遺伝子は 5 クラスに分類され、患者群(紫色)は健常者群(紺色)から分離され、4 サブグループ A(緑色), B(水色), C(赤色), D(橙色)に分類された。文献 6 より引用改変。

文献

1) Bielekova B, Martin R: Development of biomarkers in multiple sclerosis. *Brain* 2004; **127**: 3225-3232

2) Fletcher JM, Lalor SJ, Sweeney CM, *et al.*: T cells in multiple sclerosis and experimental autoimmune encephalomyelitis. *Clin Exp Immunol* 2010; **162**: 1-11

3) McFarland HF, Martin R: Multiple sclerosis: a complicated picture of autoimmunity. *Nat Immunol* 2007; **8**: 913-919

4) Durelli L, Conti L, Clerico M, *et al.*: T-helper 17 cells expand in multiple sclerosis and are inhibited by interferon-β. *Ann Neurol* 2009; **65**: 499-509

5) Axtell RC, de Jong BA, Boniface K, *et al.*: T helper type 1 and 17 cells determine efficacy of interferon-β in multiple sclerosis and experimental encephalomyelitis. *Nat Med* 2010; **16**: 406-412

6) Zozulya AL, Wiendl H: The role of regulatory T cells in multiple sclerosis. *Nat Clin Pract Neurol* 2008; **4**: 384-398

7) Friese MA, Fugger L: Pathogenic $CD8^+$ T cells in multiple sclerosis. *Ann Neurol* 2009; **66**: 132-141

8) Dalakas MC: B cells as therapeutic targets in autoimmune neurological disorders. *Nat Clin Pract Neurol* 2008; **4**: 557-567

9) Vyshkina T, Kalman B: Autoantibodies and neurodegeneration in multiple sclerosis. *Lab Invest* 2008; **88**: 796-807

10) Satoh J: Bioinformatics approach to identifying molecular biomarkers and networks in multiple sclerosis. *Clin Exp Neuroimmunol* 2010; **1**: 127-140

図の説明

図 1. MS 病態形成に関与するリンパ球. イタリックは主要な転写因子を示す。文献 2 より引用改変。

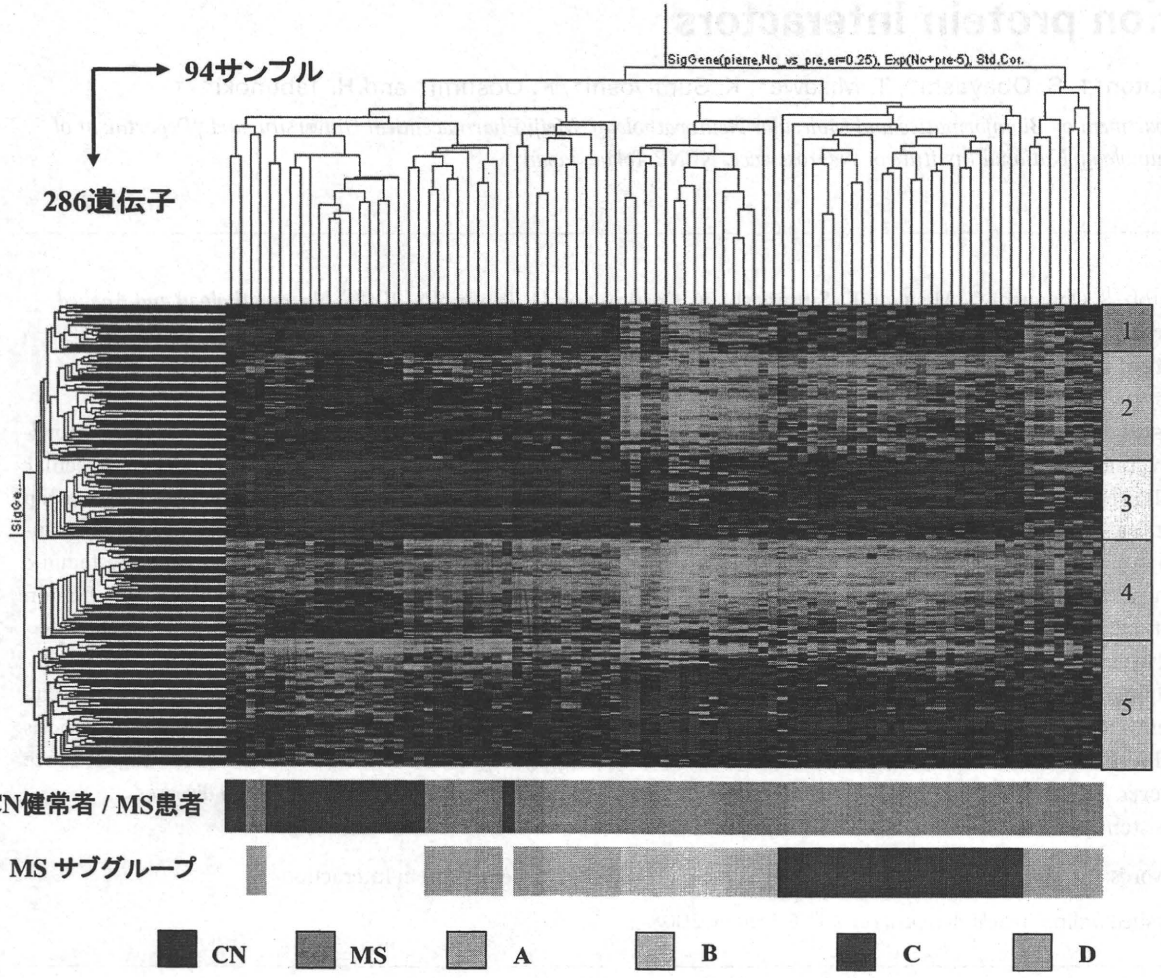
94サンプル
286遺伝子
SigGene(pierre,Nc_vs_pre,er=0.25), Exp(Nc+pre-5), Std.Cor.
1
2
3
4
5
CN健常者 / MS患者
MS サブグループ
CN
MS
A
B
C
D

図1

Neuropathology and Applied Neurobiology (2009), **35**, 16–35 doi: 10.1111/j.1365-2990.2008.00947.x

Protein microarray analysis identifies human cellular prion protein interactors

J. Satoh*†, S. Obayashi*, T. Misawa*, K. Sumiyoshi*, K. Oosumi* and H. Tabunoki*

**Department of Bioinformatics and Molecular Neuropathology, Meiji Pharmaceutical University, and †Department of Immunology, National Institute of Neuroscience, NCNP, Tokyo, Japan*

J. Satoh, S. Obayashi, T. Misawa, K. Sumiyoshi, K. Oosumi and H. Tabunoki (2009) *Neuropathology and Applied Neurobiology* **35**, 16–35

Protein microarray analysis identifies human cellular prion protein interactors

Aims: To obtain an insight into the function of cellular prion protein (PrPC), we studied PrPC-interacting proteins (PrPIPs) by analysing a protein microarray. **Methods:** We identified 47 novel PrPIPs by probing an array of 5000 human proteins with recombinant human PrPC spanning amino acid residues 23–231 named PR209. **Results:** The great majority of 47 PrPIPs were annotated as proteins involved in the recognition of nucleic acids. Coimmunoprecipitation and cell imaging in a transient expression system validated the interaction of PR209 with neuronal PrPIPs, such as FAM64A, HOXA1, PLK3 and MPG. However, the interaction did not generate proteinase K-resistant proteins. KeyMolnet, a bioinformatics tool for analysing molecular interaction on the curated knowledge database, revealed that the complex molecular network of PrPC and PrPIPs has a significant relationship with AKT, JNK and MAPK signalling pathways. **Conclusions:** Protein microarray is a useful tool for systematic screening and comprehensive profiling of the human PrPC interactome. Because the network of PrPC and interactors involves signalling pathways essential for regulation of cell survival, differentiation, proliferation and apoptosis, these observations suggest a logical hypothesis that dysregulation of the PrPC interactome might induce extensive neurodegeneration in prion diseases.

Keywords: cellular prion protein, KeyMolnet, protein microarray, protein–protein interaction

Published online *Article Accepted* on 23th February 2008

Introduction

Prion diseases are a group of neurodegenerative disorders affecting both animals and humans [1,2]. The great majority of prion diseases are transmissible, and characterized by intracerebral accumulation of an abnormal prion protein (PrPSc) that is identical in amino acid sequence to the cellular isoform (PrPC) encoded by the *PRNP* gene. PrPC is expressed widely in neural and non-neural tissues at the highest level in neurones in the central nervous system (CNS) [3]. PrPSc differs biochemically from PrPC by its β sheet-enriched structure, detergent insolubility, limited proteolysis by proteinase K, a slower turnover rate and infectivity. Previous studies suggested that the protein conformational conversion of α-helix-rich PrPC into β sheet-rich PrPSc involves a homotypic interaction between endogenous PrPC and incoming or *de novo* generated PrPSc via a post-translational process mediated by as yet unidentified species-specific auxiliary factor(s) named 'protein X' [4,5].

At present, the biological function of PrPC remains largely unknown. Several lines of PrPC-deficient mice were established independently by different gene-targeting strategies [6–8]. All of them exhibited normal early development and complete protection against scrapie infection. These observations indicate that PrPC is dispensable for embryonic development, but is pivotal for inducing prion

Correspondence: Jun-ichi Satoh, Department of Bioinformatics and Molecular Neuropathology, Meiji Pharmaceutical University, 2-522-1 Noshio, Kiyose, Tokyo 204–8588, Japan. Tel: +81 42 4958678; Fax: +81 42 4958678; E-mail: satoj@my-pharm.ac.jp

diseases. Several *in vitro* studies suggested a role of PrPC in neuritogenesis [9,10], neuronal cell adhesion [11] and a receptor for neurotrophic factors [12]. More consistently, many studies indicated that an octapeptide repeat region of PrPC with a copper-binding capacity exhibits an antioxidant activity [13]. However, none of previous findings provided an adequate explanation for mild phenotypes of PrPC-deficient mice.

A number of previous studies, by employing mainly the yeast two-hybrid (Y2H) screening system, identified a wide variety of PrPC-interacting proteins (PrPIPs). They include synapsin I [14], glial fibrillary acidic protein [15], amyloid precursor-like protein 1 [16], heat shock protein Hsp60 [17–19], the Hsp cofactor STI-1 [20], the antiapoptotic molecule Bcl-2 [21], signal-transducing adapters such as Grb2 [14], ZAP70 [22] and 14-3-3 [23], neurotrophin receptor interacting MAGE homolog [24], tubulin [25], heterogeneous ribonuclear protein A2/B1 [26], casein kinase 2 [27], plasminogen [28], laminin receptor precursor [29], laminin [9] and vitronection [30]. Most of these molecules play a key role in signal-transducing events essential for neuronal function. However, none of them could serve as the chaperone 'protein X'.

The Y2H system is a powerful approach to identify novel protein–protein interactions. However, Y2H screening requires a lot of time and effort, and is often criticized for detecting the interactions unrelated to the physiological setting, and obtaining high rates of false positive interactors caused by spontaneous activation of reporter genes and self-activating bait proteins [31,32]. Recently, protein microarray technology has been established for rapid, systematic and less expensive screening of thousands of protein–protein interactions in a high-throughput fashion [33,34]. The array includes numerous protein targets of various functional classes immobilized on a single glass slide. The protein microarray has important applications in the areas not only of basic biological research on a whole-proteome scale, but also of drug discovery research of target identification [35,36].

In order to establish a therapeutic intervention targeted on prion propagation, it is essential to clarify the biological function of PrPC and the pathological implication of PrPSc, and equally important to identify all human PrPIPs, some of which potentially serve as a candidate for 'protein X'. The present study was designed to identify a comprehensive profile of the human PrPC interactome by analysing a high-density protein microarray, and to obtain an insight into the PrPC–PrPIPs network.

Materials and methods

Preparation of a V5-tagged PrP probe for microarray analysis

Human embryonic kidney cells HEK293, whose genome was modified for the Flp-In system (Flp-In 293; Invitrogen, Carlsbad, CA), contain a single Flp recombination target (FRT) site targeted for the site-specific recombination, integrated in a transcriptionally active locus of the genome, where it stably expresses the *lacZ*–Zeocin fusion gene driven from the pFRT/*lac*Zeo plasmid under the control of SV40 early promoter. The cells were maintained in Dulbecco's modified Eagle's medium supplemented with 10% foetal bovine serum, 100 U/ml penicillin and 100 μg/ml streptomycin (feeding medium) with inclusion of 100 μg/ml zeocin, as described previously [37].

To prepare the probe for protein microarray analysis, the gene encoding a truncated form of human PrPC spanning amino acid residues 23–231 named PR209 was amplified by polymerase chain reaction (PCR) using Pfu-Turbo DNA polymerase (Stratagene, La Jolla, CA) and the primer sets listed in Table S1 online. The PCR product was then cloned into a mammalian expression vector pSecTag/FRT/V5-His TOPO (Invitrogen) to produce a fusion protein with a C-terminal V5 tag, a C-terminal polyhistidine (6xHis) tag and an N-terminal Ig κ-chain secretion signal. This vector, together with the Flp recombinase expression vector pOG44 (Invitrogen), was transfected in Flp-In 293 cells by Lipofectamine 2000 reagent (Invitrogen). A stable cell line was established after incubating the transfected cells for 1 month in the feeding medium with inclusion of 100 μg/ml hygromycin B. In this system, the recombinant protein was secreted into the culture medium after the Ig κ-chain secretion signal sequence was processed by an endogenous signal peptidase-mediated cleavage.

To purify the V5-tagged PR209 protein, the serum-free culture supernatant was harvested, and concentrated at a 1/40 volume by centrifugation on an Amicon Ultra-15 filter (Millipore, Bedford, MA). It was then purified by the HIS-select spin column (Sigma, St. Louis, MO), and concentrated at a 1/10 volume by centrifugation on a Centricon-10 filter (Millipore). The protein concentration was determined by a Bradford assay kit (Bio-Rad, Hercules, CA). The purity and specificity of the probe were verified by Western blot analysis using mouse monoclonal anti-V5 antibody (Invitrogen), mouse monoclonal anti-

PrP antibody 3F4 (Dako, Tokyo, Japan) and rabbit polyclonal antibody C20 specific for the sequence close to the C-terminus of PrPC (Santa Cruz Biotechnology, Santa Cruz, CA). To determine the status of glycosylation, 5 μg of the probe protein was deglycosylated by incubating it at 37°C for 1.5 h with 5000 U peptide N-glycosidase F (New England BioLabs, Beverly, MA), followed by separation on the gel [37].

Protein microarray analysis

The present study utilized the ProtoArray human protein microarray v3.0 (Invitrogen). It contains approximately 5000 recombinant GST-tagged human proteins expressed by the baculovirus expression system and purified under native conditions by using gluthathione affinity chromatography to ensure the preservation of native structure, post-translational modifications and proper functionality of target proteins [36,38]. They were spotted in duplicate on a nitrocellulose-coated glass slide. The target proteins cover a wide range of biologically important proteins selected from the human ultimate open reading frame (ORF) clone collection (Invitrogen). The probe is spatially accessible to all parts of target proteins on the array, which protrude from the glass slide surface via the N-terminal GST fusion tag serving as a spacer. The complete list is shown in Table S2 online. The proteins are spotted in an arrangement of 4 × 12 subarrays equally spaced in vertical and horizontal directions. Each subarray includes 20 × 20 spots, composed of 76 positive and negative control spots (C), 222 human target proteins (H), and 102 blanks and empty spots (B) (Figure 1b). The 14 positive control spots include four of an Alexa Fluor 647-labelled antibody (row 1, columns 1, 2; row 14, columns 13, 14), six of a concentration gradient of a biotinylated anti-mouse antibody with a capacity to bind to mouse monoclonal anti-V5 antibody conjugated with Alexa Fluor 647 (row 14, columns 15–20), and four of a concentration gradient of V5 protein (row 15, columns 5–8). The 62 negative control spots include six of a concentration gradient of bovine serum albumin (BSA) (row 1, columns 3–8), four of a concentration gradient of a rabbit anti-GST antibody (row 1, columns 9–12), four of a concentration gradient of calmodulin (row 1, columns 13–16), 16 of a concentration gradient of GST (row 1, columns 17–20; row 2, columns 1–12), 10 of buffer only (row 15, columns 1, 2, 9–16), eight of human IgG subclasses (row 15, columns 17–20; row 16, columns 1–4), 12 of Invitrogen internal controls (row 4, columns 9, 10; row 6, columns 15–18; row 7, columns 9, 10, 15, 16; row 8, columns 13, 14), and two of an antibiotin antibody (row 15, columns 3, 4).

Non-specific binding was blocked by incubating the array for 90 min in the PBST blocking buffer composed of 1% BSA and 0.1% Tween 20 in phosphate-buffered saline (PBS). Then, it was incubated for 30 min at 4°C with the probe described above at a concentration of 200 μg/ml in the probing buffer composed of 1% BSA, 5 mM $MgCl_2$, 0.5 mM dithiothreitol, 0.05% Triton X-100 and 5% glycerol in PBS. The array was washed three times with the probing buffer, and then incubated for 30 min at 4°C with mouse monoclonal anti-V5 antibody labelled with Alexa Fluor 647 (Invitrogen) at a concentration of 260 ng/ml in the probing buffer. Then, the array was washed three times with the probing buffer, and scanned by the GenePix 4200 A scanner (Axon Instruments, Union City, CA) at a wavelength of 635 nm. The data were analysed by using the ProtoArray Prospector software v3.0 (Invitrogen), following acquisition of the microarray lot-specific information, which compensates inter-lot variations in protein concentrations identified by the post-printing quality control. According to the manufacturer-recommended setting of the ProtoArray Prospector software, the spots showing the background-subtracted signal intensity value greater than the median plus three standard deviations of all the fluorescence intensities were considered as having significant interactions. The Z-score, an indicator for statistical significance of binding specificity, was calculated as the background-subtracted signal intensity value of the target protein minus the average of the background-subtracted signal intensity value from the negative control distribution, divided by the standard deviation of the negative control distribution.

Bioinformatics analysis

The gene expression pattern of mouse orthologues of PrPIPs in the brain was searched on the Allen Brain Atlas database [39], an anatomically comprehensive digital atlas containing the expression patterns of more than 20 000 genes in the adult mouse brain analysed by high-throughput *in situ* hybridization methods (http://www.brain-map.org).

The interaction of PrPC with PrPIPs was searched on the Biomolecular Interaction Network database (BIND) (http://bond.unleashedinformatics.com). Functional

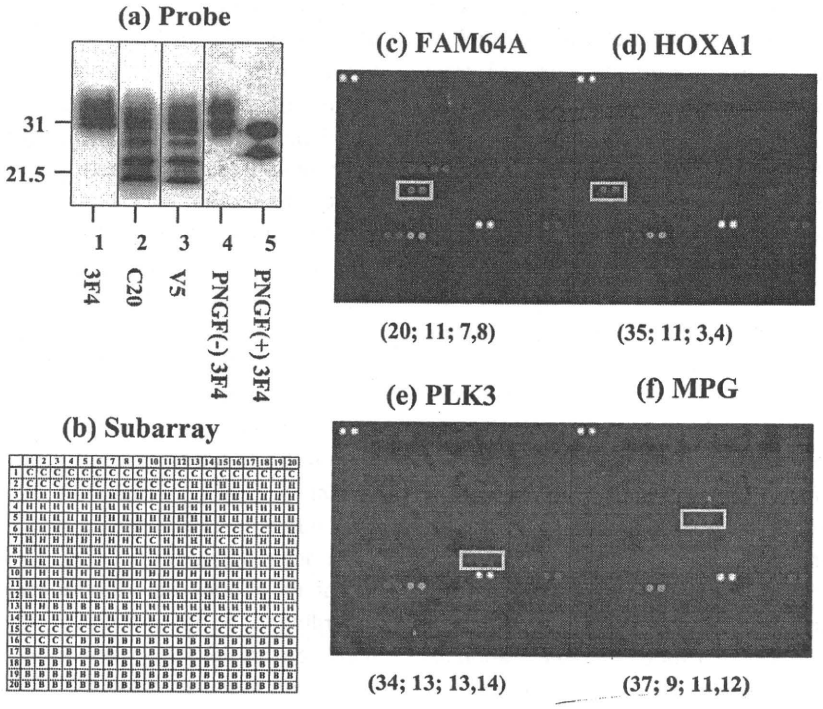

Figure 1. Protein microarray analysis. (a) Western blot of PR209 probe. The lanes (1–5) represent the immunolabelling with the antibodies following: (1) 3F4, (2) C20, (3) V5, (4) 3F4 before treatment with peptide N-glycosidase F (PNGase F) and (5) 3F4 after treatment with PNGase F. (b) The layout of subarray. The high-density protein microarray (5000 proteins, duplicate spots each) utilized in the present study contains 4 × 12 subarrays. Each subarray includes 20 × 20 spots. They are composed of 76 control spots (C) including 14 positive and 62 negative control spots, 222 human target proteins (H) and 102 blanks and empty spots (B), as described in *Materials and methods*. (c) FAM64A. The spot location is subarray 20, row 11, columns 7, 8. (d) HOXA1. Subarray 35, row 11, columns 3, 4. (e) PLK3. Subarray 34, row 13, columns 13, 14. (f) MPG. Subarray 37, row 9, columns 11, 12. PR209 interactors located on different subarrays (c–f) are indicated by an enclosed yellow line. It is worthy to note that in each subarray, positive control spots composed of an Alexa Fluor 647-labelled antibody (row 1, columns 1, 2; row 14, columns 13, 14), a concentration gradient of a biotinylated anti-mouse antibody with a capacity to bind to mouse monoclonal anti-V5 antibody conjugated with Alexa Fluor 647 (row 14, columns 15–20; signals visible on the higher concentration), and a concentration gradient of V5 protein (row 15, columns 5–8; signals visible on the higher concentration) are identified as positive, whereas negative control spots composed of a concentration gradient of BSA (row 1, columns 3–8), a concentration gradient of a rabbit anti-GST antibody (row 1, columns 9–12), a concentration gradient of calmodulin (row 1, columns 13–16), a concentration gradient of GST (row 1, columns 17–20; row 2, columns 1–12), buffer only (row 15; columns 1, 2, 9–16), human IgG subclasses (row 15, columns 17–20; row 16, columns 1–4), Invitrogen internal controls (row 4, columns 9, 10; row 6, columns 15–18; row 7, columns 9, 10, 15, 16; row 8, columns 13, 14), and an antibiotin antibody (row 15, columns 3, 4) are found as negative.

annotation of PrPIPs was searched by the web-accessible program named Database for Annotation, Visualization and Integrated Discovery (DAVID) version 2007, National Institute of Allergy and Infectious Diseases, National Institutes of Health (NIH) (http://david.abcc.ncifcrf.gov) [40]. It covers more than 40 annotation categories, including Gene Ontology terms, protein–protein interactions, protein functional domains, disease associations, biological pathways, sequence general features, homologies, gene functional summaries and tissue expressions. By importing the list of Entrez gene IDs of PrPIPs, this program creates the functional annotation chart, an annotation term-focused view that lists annotation terms and their associated genes under study. To avoid excessive counting of duplicated genes, the Fisher's exact statistics is calculated based on corresponding DAVID gene IDs by which all redundancies in original IDs are removed.

The molecular network of PrPIPs was analysed by the software named KeyMolnet (Institute of Medicinal Molecular Design, Tokyo, Japan) [41]. It operates on a comprehensive knowledge database, composed of information on relationships among human genes, molecules, diseases, pathways and drugs, carefully curated by expert biologists from review articles, literature and public

databases. They are categorized into the core contents collected from selected review articles with the highest reliability or the secondary contents extracted from abstracts of PubMed database and Human Reference Protein database.

By importing the list of Entrez gene IDs, KeyMolnet automatically provides corresponding molecules as a node on networks [41,42]. Among various network-searching algorithms, the 'N-points to N-points' search extracts the molecular network with the shortest route connecting the starting-point molecules and the end-point molecules. The generated network was compared side by side with 346 human canonical pathways of the KeyMolnet library. The algorithm counting the number of overlapping molecular relations between the extracted network and the canonical pathway makes it possible to identify the canonical pathway showing the most significant contribution to the extracted network. The significance in the similarity between both is scored following the formula, where O = the number of overlapping molecular relations between the extracted network and the canonical pathway, V = the number of molecular relations located in the extracted network, C = the number of molecular relations located in the canonical pathway, T = the number of total molecular relations (approximately 90 000 sets) and X = the sigma variable that defines incidental agreements.

$$\text{score} = -\log_2\left(\sum_{x=O}^{Min(C,V)} f(x)\right)$$

$$f(x) = {}_{C}C_{X} \cdot {}_{T-C}C_{V-x} / {}_{T}C_{V}$$

Immunoprecipitation and Western blot analysis

PR209, the N-terminal half of PR209 (amino acid residues 23–121), the C-terminal half of PR209 (amino acid residues 122–231), and the ORF of family with sequence similarity 64, member A (FAM64A), polo-like kinase 3 (PLK3), N-methylpurine-DNA glycosylase (MPG) and homeobox A1 (HOXA1) were amplified by PCR using PfuTurbo DNA polymerase and the primer sets listed in Table S1 online. They were then cloned into the mammalian expression vector p3XFLAG-CMV7.1 (Sigma) or pCMV-Myc (Clontech, Mountain View, CA) to express a fusion protein with an N-terminal Flag or Myc tag. At 48 h after co-transfection of the vectors, HEK293 cells were homogenized in M-PER lysis buffer (Pierce, Rockford, IL) supplemented with a cocktail of protease inhibitors (Sigma). In limited experiments, a proteasome inhibitor MG-132 (Merck-Calbiochem, Tokyo, Japan) was added at a final concentration of 10 μM in the culture medium during the last 24 h before harvest. After preclearance, the supernatant was incubated at 4°C for 3 h with mouse monoclonal anti-Flag M2 affinity gel (Sigma), rabbit polyclonal anti-Myc-conjugated agarose (Sigma) or the same amount of normal mouse or rabbit IgG-conjugated agarose (Santa Cruz Biotechnology). After several washes, the immunoprecipitates were processed for Western blot analysis using rabbit polyclonal anti-Myc antibody (Sigma) and mouse monoclonal anti-FLAG M2 antibody (Sigma). The specific reaction was visualized using a chemiluminescence substrate (Pierce).

To determine the proteinase K-resistant property of PR209, the cells were homogenized in M-PER lysis buffer without inclusion of protease inhibitors. The protein extract was then incubated at 37°C for 30 min with 5 μg/ml recombinant proteinase K (Roche Diagnostics, Mannheim, Germany), followed by adding phenylmethylsulphonyl fluoride at a final concentration of 5 mM, according to the methods described previously [43]. Proteins were precipitated by adding 6% trichloroacetic acid. After centrifugation at 4°C for 15 min at 16 100 g, the pellets were washed with cold acetone, and processed for Western blot analysis using 3F4 antibody.

To determine the detergent-insoluble property of PR209, the cells were homogenized in a lysis buffer containing 100 mM NaCl, 10 mM EDTA, 10 mM Tis (pH 7.4), 0.5% Nonidet P-40 and 0.5% sodium deoxycholate, according to the methods described previously [44]. The lysate was centrifuged at 4°C for 10 min at 2000 g to remove debris. Then, the supernatant was further centrifuged at 4°C for 1 h at 16 100 g to separate detergent-soluble (supernatant) and detergent-insoluble (pellet) fractions. They were processed for Western blot analysis using 3F4 antibody. HRP-conjugated secondary antibodies were obtained from Santa Cruz Biotechnology.

Cell imaging analysis

PR209 and the ORF of FAM64A, PLK3, MPG and HOXA1 were amplified by PCR using PfuTurbo DNA polymerase and the primer sets listed in Table S1 online. They were then cloned into the mammalian expression vector pDsRed-Express-C1 (Clontech), pEYFP-C1 (Clontech), pcDNA3.1/NT/GFP-TOPO (Invitrogen) or pcDNA3.1/CT/GFP-TOPO (Invitrogen) to express a fusion protein with an N-terminal or C-terminal DsRed, EYFP or GFP tag. At 24–48 h after co-transfection of the vectors, the cells were

fixed briefly in 4% paraformaldehyde, mounted on slides with glycerol-polyvinyl alcohol, and examined on the Olympus BX51 universal microscope.

Human neural cell lines and cultures

Human astrocytes (AS) in culture were established from neuronal progenitor (NP) cells of human foetal brain (Cambrex, Walkersville, MD). For the induction of neuronal differentiation, NTera2 cells maintained in the undifferentiated state (NTera2-U) were incubated for 4 weeks in feeding medium containing 10^{-5} M *all trans* retinoic acid (Sigma), replated twice and then plated on a surface coated with Matrigel Basement Membrane Matrix (Becton Dickinson, Bedford, MA). They were incubated for another 2 weeks in feeding medium containing a cocktail of mitotic inhibitors, resulting in the enrichment of differentiated neurones (NTera2-N), as described previously [45]. Human microglia cell line HMO6 was provided by Dr Seung U. Kim, Division of Neurology, University of British Columbia, Vancouver, B.C., Canada. Total RNA of the human frontal cerebral cortex was obtained from Clontech.

Reverse transcription-PCR analysis

DNase-treated total cellular RNA was processed for cDNA synthesis using oligo$(dT)_{12-18}$ primers and SuperScript II reverse transcriptase (Invitrogen). Then, cDNA was amplified by PCR using HotStar Taq DNA polymerase (Qiagen, Valencia, CA) and a panel of primer sets listed in Table S1 online. The amplification program consisted of an initial denaturing step at 95°C for 15 min, followed by a denaturing step at 94°C for 1 min, an annealing step at 60°C for 40 s and an extension step at 72.9°C for 50 s for 30–35 cycles, except for the glyceraldehyde-3-phosphate dehydrogenase (G3PDH), an internal control, amplified for 27 cycles.

Results

Protein microarray analysis identified 47 novel PrPC interactors

To analyse the human protein microarray, V5-tagged PR209 probe was purified from the supernatant of a stable cell line secreting the recombinant protein in the culture medium. By Western blot analysis, the probe was composed of a mixture of glycosylated full-length and N-terminally truncated forms of PrPC (Figure 1a, lanes 1–5). The 18.5-kDa protein identified by C20 but not by 3F4 represents the C-terminal fragment produced by constitutive metalloprotease-mediated cleavage [46]. Among total 5000 proteins on the array, 47 were identified as the proteins showing significant interaction with the probe (Table 1). They include FAM64A (Figure 1c), HOXA1 (Figure 1d), casein kappa (CSN3), bromodomain adjacent to zinc finger domain, 2B (BAZ2B), chromosome 7 ORF 50 (C7orf50), surfeit 2 (SURF2), sodium channel modifier 1 (SCNM1), chromosome 18 ORF 56 (C18orf56), PLK3 (Figure 1e), RNA binding motif protein 22 (RBM22), hypothetical protein DKFZp761B107, MPG (Figure 1f), zinc finger protein 192 (ZNF192), thymic stromal lymphopoietin (TSLP), DEAD box polypeptide 47 (DDX47), MAP/microtubule affinity-regulating kinase 4 (MARK4), zinc finger protein 408 (ZNF408), TBP-like 1 (TBPL1), activator of basal transcription 1 (ABT1), ribosomal protein L41 (RPL41), zinc finger protein 740 (ZNF740), CWC15 homolog, four and a half LIM domains 1 (FHL1), amyotrophic lateral sclerosis 2 chromosome region, candidate 4 (ALS2CR4), immediate early response 3 (IER3), KIAA1191, peptidyl-tRNA hydrolase 1 homolog (PTRH1), phosphodiesterase 4D interacting protein (PDE4DIP), Rho GTPase activating protein 15 (ARHGAP15), mitochondrial GTPase 1 homolog (MTG1), cirrhosis, autosomal recessive 1 A (CIRH1A), eukaryotic translation initiation factor 2C, 1 (EIF2C1), WD repeat domain 5 (WDR5), centaurin, alpha 2 (CENTA2), protein phosphatase 1, regulatory subunit 14 A (PP1R14 A), cold inducible RNA binding protein (CIRBP), zinc finger, FYVE domain containing 28 (ZFYVE28), within bgcn homolog (WIBG), nucleolar protein family A, member 2 (NOLA2), PTPRF interacting protein, binding protein 2 (PPFIBP2), family with sequence similarity 27, member E3 (FAM27E3), fibroblast growth factor 13 (FGF13), apoptosis-inducing factor, mitochondrion-associated, 3 (AIFM3), 2′,3′-cyclic nucleotide 3′ phosphodiesterase (CNP), NIN1/RPN12 binding protein 1 homolog (NOB1), RNA-binding region containing 3 (RNPC3) and dual-specificity tyrosine-phosphorylation regulated kinase 3 (DYRK3). The gene expression pattern of PrPC interactors (PrPIPs) in the adult brain analysed by *in situ* hybridization was searched on the Allen Brain Atlas database [39]. Among 47 PrPIPs, at least 35 mouse orthologues (74%) were expressed in various regions of the adult mouse brain (Table 1). The expression pattern of the remaining

Table 1. PrPC-interacting proteins (PrPIPs) identified by protein microarray analysis

No.	*Entrez gene ID*	*Gene symbol*	*Gene name*	*Putative molecular function*	*Block*	*Row*	*Column*	*Z-score*	*Gene expression in adult mouse brain (region with the highest expression level)*
1	54478	FAM64A	Family with sequence similarity 64, member A	A protein with the DUF1466 domain of unknown function	20	11	7, 8	21.89656	Unknown
2	3198	HOXA1	Homeobox A1	A transcription factor that regulates the placement of hindbrain segments in the proper location along the anterior–posterior axis during development	35	11	3, 4	18.36074	Yes (CB)
3	1448	CSN3	Casein kappa	A milk protein	20	9	9, 10	12.58106	Yes (OLF)
4	29994	BAZ2B	Bromodomain adjacent to zinc finger domain, 2B	A component of chromatin remodeling complexes	24	10	5, 6	7.96988	Yes (MY)
5	84310	C7orf50	Chromosome 7 open reading frame 50	A hypothetical protein of unknown function	21	11	9, 10	6.7938	Unknown
6	6835	SURF2	Surfeit 2	The housekeeping gene of unknown function	15	9	15, 16	6.31368	Yes (MY)
7	79005	SCNM1	Sodium channel modifier 1	A zinc finger protein acting as a premRNA splicing factor	18	6	3, 4	6.06453	Yes (CB and other regions)
8	494514	C18orf56	Chromosome 18 open reading frame 56	A hypothetical protein of unknown function	10	10	19, 20	6.02515	Unknown
9	1263	PLK3	Polo-like kinase 3 (Drosophila)	A serine/threonine kinase that regulates cell cycle progression	34	13	13, 14	5.94109	Yes (MY)
10	55696	RBM22	RNA binding motif protein 22	A zinc finger protein with the RNA recognition motif of unknown function	20	9	7, 8	5.67225	Yes (CB)
11	91050	DKFZp761B107	Hypothetical protein DKFZp761B107	A protein with the SMC N-terminal domain of unknown function	22	12	3, 4	5.36251	Unknown
12	4350	MPG	N-methylpurine-DNA glycosylase	A DNA glycosylase acting as a DNA repair enzyme	37	9	11, 12	5.16637	Yes (RHP)
13	7745	ZNF192	Zinc finger protein 192	A Kruppel family zinc finger transcription factor	21	11	13, 14	5.12927	Unknown
14	85480	TSLP	Thymic stromal lymphopoietin	A haemopoietic cytokine that enhances the maturation of dendritic cells	21	10	19, 20	4.92555	Yes (RHP)
15	51202	DDX47	DEAD (Asp-Glu-Ala-Asp) box polypeptide 47	A member of the DEAD box protein family RNA helicases	2	11	11, 12	4.90132	Yes (MY)
16	57787	MARK4	MAP/microtubule affinity-regulating kinase 4	A serine/threonine kinase that regulates microtubule organization in neuronal cells	12	13	5, 6	4.38333	Yes (TH)
17	79797	ZNF408	Zinc finger protein 408	A zinc finger protein with the SFP1 domain acting as a transcriptional repressor that regulates cell cycle	21	11	19, 20	4.27504	Unknown

18	9519	TBPL1	TBP-like 1	A general transcription factor that regulates spermatogenesis	3	12	1, 2	4.16447	Yes (OLF)
19	29777	ABT1	Activator of basal transcription 1	A basal transcriptional activator	36	9	15, 16	3.97136	Yes (OLF)
20	6171	RPL41	Ribosomal protein L41	A componet of the 60S ribosome subunit	14	10	7, 8	3.9388	Unknown
21	283337	ZNF740	Zinc finger protein 740	A zinc finger protein of unknown function	20	9	15, 16	3.88503	Unknown
22	51503	CWC15	CWC15 homolog (S. cerevisiae)	A cell cycle control protein involved in mRNA splicing	19	7	13, 14	3.78582	Unknown
23	2273	FHL1	Four and a half LIM domain 1	A protein with the LIM domain that regulates skeletal muscle differentiation	26	3	11, 12	3.75175	Yes (sAMY)
24	65062	ALS2CR4	Amyotrophic lateral sclerosis 2 (juvenile) chromosome region, candidate 4	A membrane protein of unknown function	34	7	7, 8	3.69722	Yes (RHP)
25	8870	IER3	Immediate early response 3	The immediate early gene acting as an antiapoptosis regulator	26	10	13, 14	3.6018	Yes (CB)
26	57179	KIAA1191	KIAA1191	A cytoplasmic protein of unknown function	10	10	13, 14	3.56924	Unknown
27	138428	PTRH1	Peptidyl-tRNA hydrolase 1 homolog (S. cerevisiae)	A peptidyl-tRNA hydrolase	47	10	19, 20	3.55258	Yes (CTX)
28	9659	PDE4DIP	Phosphodiesterase 4D interacting protein (myomegalin)	A protein of the golgi/centrosome that interacts with a cyclic nucleotide phosphodiesterase	25	11	1, 2	3.54046	Yes (HIP)
29	55843	ARHGAP15	Rho GTPase activating protein 15	A Rho GTPase-activating protein acting as a regulator of RAC1	9	6	13, 14	3.50411	Yes (CTX)
30	92170	MTG1	Mitochondrial GTPase 1 homolog (S. cerevisiae)	A mitochondrial GTPase	48	14	7, 8	3.49729	Yes (HIP)
31	84916	CIRH1A	Cirrhosis, autosomal recessive 1 A (cirhin)	A mitochondrial protein with WD40 repeats of unknown function	14	10	19, 20	3.4511	Yes (HIP)
32	26523	EIF2C1	Eukaryotic translation initiation factor 2C, 1	A member of the Argonaute family (AGO1) that plays a role in siRNA-mediated gene silencing	18	11	11, 12	3.43671	Yes (HIP)
33	11091	WDR5	WD repeat domain 5	A protein with WD40 repeats that constitutes a component of histone methyltransferase complexes	20	7	9, 10	3.37083	Yes (HIP)
34	55803	CENTA2	Centaurin, alpha 2	A plasma membrane GTPase activating protein with PH domains	47	12	5, 6	3.25269	Yes (MY)
35	94274	PPP1R14 A	Protein phosphatase 1, regulatory (inhibitor) subunit 14 A	A phosphorylation-dependent inhibitor of smooth muscle myosin phosphatase	9	5	3, 4	3.25117	Yes (MY)
36	1153	CIRBP	Cold-inducible RNA binding protein	A cold stress-inducible protein wuth the RNA recognition motif that plays a role in cold-induced suppression of cell proliferation	16	10	3, 4	3.22391	Yes (CTX)

Table 1. (*Continued*)

No.	Entrez gene ID	Gene symbol	Gene name	Putative molecular function	Block	Row	Column	Z-score	Gene expression in adult mouse brain (region with the highest expression level)
37	57732	ZFYVE28	Zinc finger, FYVE domain containing 28	An endosomal protein with the FYVE domain that targets proteins to membrane lipids via interaction with PI3P	12	10	11,12	3.20574	Yes (CB and other regions)
38	84305	WIBG	Within bgcn homolog (Drosophila)	A protein with the Mogo-bind domain of unknown function	43	9	15,16	3.19741	Yes (OLF)
39	55651	NOLA2	Nucleolar protein family A, member 2 (H/ACA small nucleolar RNPs)	A member of the H/ACA snoRNPs gene family that regulates rRNA processing and modification	15	6	15,16	3.155	Yes (OLF)
40	8495	PPFIBP2	PTPRF interacting protein, binding protein 2 (liprin beta 2)	A protein with SAM domains acting as a scaffold for recruitment and anchoring of LAR family PTPases	47	12	11,12	3.13682	Yes (MY)
41	286301	FAM27E3	Family with sequence similarity 27, member E3	A protein of unknown function	14	11	9,10	3.11032	Unknown
42	2258	FGF13	Fibroblast growth factor 13	A member of the FGF family that plays a role in neuronal development	35	11	17,18	3.1035	Yes (HIP)
43	150209	AIFM3	Apoptosis-inducing factor, mitochondrion-associated, 3	A mitochondrial protein with the Rieske domain and the pyridine nucleotide-disulphide oxidoreductase domain acting as an apoptosis inducer	42	10	15,16	3.09063	Unkown
44	1267	CNP	2′,3′-cyclic nucleotide 3′ phosphodiesterase	A cyclic nucleotide phosphodiesterase serving as a marker of myelin	20	10	19,20	3.07624	Yes (CB and other regions)
45	28987	NOB1	NIN1/RPN12 binding protein 1 homolog (S. cerevisiae)	A protein with the PUN domain and the zinc ribbon domain acting as a ribonuclease	14	11	17,18	3.06336	Yes (CB and other regions)
46	55599	RNPC3	RNA-binding region (RNP1, RRM) containing 3	A nuclear protein with RNA recognition motifs that constitutes a component of the U12-type spliceosome	9	8	19,20	3.01035	Yes (OLF)
47	8444	DYRK3	Dual-specificity tyrosine-(Y)-phosphorylation regulated kinase 3	A DYRK family dual-specificity protein kinase that regulates caveolae trafficking	20	13	9,10	3.00278	Yes (HIP)

Among 5000 proteins on the microarray, 47 were identified as the proteins showing a significant interaction. They are listed with Entrez Gene ID, gene symbol, gene name, molecular function, the position on the array, the Z-score and the information on gene expression in the adult mouse brain, including the region with the highest expression level on the sagittal plane of the Allen Brain Atlas.

CB, cerebellum; CTX, cerebral cortex; HIP, hippocampal region; MY, medulla oblongata; OLF, olfactory bulb; sAMY, striatum-like amygdalar nuclei; TH, thalamus; RHP, retrohippocampal region.

12 genes in the adult mouse brain is currently unknown. Thus, the expression of PrPIPs is enriched in the adult mouse brain, suggesting the possible interaction of these with PrPC that is expressed broadly at high levels in neurones of the adult rodent CNS [3]. The BIND database search indicated that none of 47 PrPIPs were classified into previously reported PrPC-interacting partners.

We did not detect any negative control spots as positive, including those of BSA, calmodulin, GST, a rabbit anti-GST antibody, human IgG subclasses, an antibiotin antibody and buffer-only control, whereas we identified a battery of positive control spots as positive, such as those of an Alexa Fluor 647-labelled antibody, a biotinylated anti-mouse antibody binding to Alexa Fluor 647-conjugated anti-V5 antibody and V5 protein (Figure 1, panels b–f). The protein microarray we utilized includes only three previously reported PrPC-binding partners, such as glial fibrillary acidic protein [15], tubulin [25] and casein kinase 2 [27] (see Table S2). However, we could not identify them as a significant PrPC interactor in the present study.

Human neurones in culture expressed mRNA of PrPC interactors

Because PrPC *in vivo* is expressed at the highest level in neurones in the CNS, it is important to identify the cell types expressing PrPIPs. By reverse transcription (RT)-PCR analysis, the transcripts coding for PRNP and PR209-interacting proteins, such as FAM64A, PLK3 and MPG, were expressed widely in various human neural and non-neural cell lines (Figure 2, panels a, c, d, e, lanes 3–12). They include cultured human AS, NP cells, NTera2 teratocarcinoma-derived differentiated neurones (NTera2N), Y79 retinoblastoma, SK-N-SH neuroblastoma, IMR-32 neuroblastoma, U-373MG astrocytoma, HMO6 microglia, HeLa cervical carcinoma and HepG2 hepatocellular carcinoma cells. In contrast, high levels of HOXA1 mRNA were expressed in limited cell types, such as NTera2N, U-373MG, HeLa and HepG2 (Figure 2, panel b, lanes 3–12). High levels of PLK3, MPG and PRNP mRNAs were also identified in the human cerebral cortex (CBR) (Figure 2, panels c, d, e, lane 1). The levels of G3PDH mRNA were constant among the cells and tissues examined (Figure 2, panel f, lanes 1, 3–12). By contrast, no products were amplified, when total RNA was processed for PCR without inclusion of the RT step, excluding a contamination of genomic DNA (Figure 2, panels a–f, lane 2). Because NTera2N cells serve as a model of differentiated human neurones in culture [45], these observations suggest that FAM64A, HOXA1, PLK3 and MPG are neuronal proteins coexpressed with PrPC.

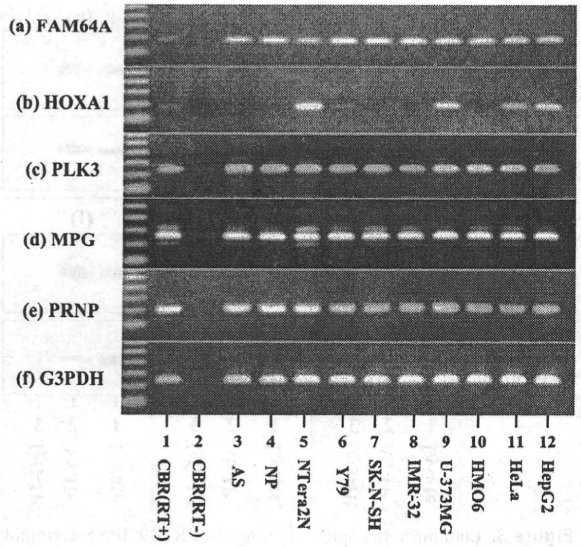

Figure 2. Expression of mRNAs of PrPC interactors in human neural cells. The expression of (a) FAM64A, (b) HOXA1, (c) PLK3, (d) MPG, (e) PRNP and (f) G3PDH mRNAs was studied in human neural and non-neural cells by RT-PCR. The lanes (1–12) represent: (1) the frontal cerebral cortex (CBR) with inclusion of the reverse transcription step (RT+), (2) CBR without inclusion of the reverse transcription step (RT–), (3) cultured astrocytes (AS), (4) cultured neuronal progenitor (NP) cells, (5) NTera2 teratocarcinoma-derived differentiated neurones (NTera2N), (6) Y79 retinoblastoma, (7) SK-N-SH neuroblastoma, (8) IMR-32 neuroblastoma, (9) U-373MG astrocytoma, (10) HMO6 microglia cell line, (11) HeLa cervical carcinoma and (12) HepG2 hepatocellular carcinoma. The DNA size marker (100-bp ladder) is shown on the left.

Validation of protein microarray data

To verify the results of protein microarray analysis, PR209 and interactors were cloned individually into distinct expression vectors, and were coexpressed transiently in HEK293 cells. FAM64A, HOXA1, PLK3 and MPG were selected for the interactors examined, because of their possible involvement in neural function (see *Discussion*). Because the antibodies suitable for immunoprecipitation with FAM64A, PLK3 and MPG are currently unavailable, we performed immunoprecipitation analysis by using the tag-specific antibodies. First, PR209 was expressed as a Flag-tagged fusion protein, whereas the interactors were

